Journal of Colloid and Interface Science **256,** 351–359 (2002)
doi:10.1006/jcis.2002.8620

Formation of Chemical Gardens

Julyan H. E. Cartwright,* Juan Manuel García-Ruiz,* María Luisa Novella,† and Fermín Otálora*

*Laboratorio de Estudios Cristalográficos, CSIC, E-18071 Granada, Spain; and †Microgravity Research Center, Universite Libre de Bruxelles, B-1050 Bruxelles, Belgium

E-mail: julyan@lec.ugr.es, jmgruiz@ugr.es, mnovella@ulb.ac.be, otalora@ugr.es

Received March 8, 2002; accepted July 17, 2002

Chemical gardens are the plant-like structures formed upon placing together a soluble metal salt, often in the form of a seed crystal, and an aqueous solution of one of many anions, often sodium silicate. We have observed the development of chemical gardens with Mach–Zehnder interferometry. We show that a combination of forced convection from osmosis and free convection from buoyancy, together with chemical reaction, is responsible for their morphogenesis. © 2002 Elsevier Science (USA)

Key Words: **chemical garden; colloidal garden; crystal garden; silica garden; silicate garden; Portland cement hydration; corrosion tubes; origin of life.**

1. INTRODUCTION

Chemical, colloidal, crystal, silica, or silicate gardens (Fig. 1) are familiar to every child with a chemistry set. As their very name indicates, their forms are similar to those observed in living organisms, which provoked a flurry of interest a century ago from investigators in search of the origin of life (1–3). Unfortunately, as the necessary notions of biochemistry were then lacking, that proved to be a false trail. However, almost a hundred years later, and several centuries on from the first observations of so-called metallic trees by the early chemists such as Glauber (38, 39), chemical gardens remain incompletely understood. In this paper we present the results of experiments observed with Mach–Zehnder interferometry designed to understand the formation and growth of the hollow tubes that are the basic structures in chemical gardens. We discuss the fluid dynamics implicated in their morphogenesis and highlight the dynamical processes underlying their characteristic patterns.

Chemical gardens are obtained from the precipitation reaction upon adding crystals of soluble metal salts to aqueous solutions containing anions such as aluminates, borates, carbonates, chromates, cyanoferrates, phosphates, or silicates (5). Alternatively, a solution of the metal salt may be used instead of the solid, when the reaction takes place at the interface between the two liquids (4, 6). Despite their chemical diversity, the common characteristic of all these reactions is the precipitation of a semipermeable colloidal membrane, across which osmosis occurs. Such precipitation membranes, first studied by Traube in the middle of the nineteenth century (7), were employed a few years later by Pfeffer in his investigations into osmosis (4) and in this way played a fundamental role in the quantitative understanding of that phenomenon, which culminated with van't Hoff's law of osmotic pressure, formulated in 1887 (8, 9).

Among all the chemical-garden reactions, those that have been most studied are from silicate solutions—hence the terms silica or silicate gardens. However, even in this case the basic mechanisms of morphogenesis remain unclear, and we choose here to study these in depth. The chemistry of sodium silicate and its behavior in solution—as water glass—is rather complex (10). Adding a crystal of a soluble metal salt to water glass provokes a reaction producing the hydrous metal silicate, which is deposited as a colloidal gel around the crystal (11). The gel acts as a semipermeable membrane, through which water and excess hydroxide ions are drawn under osmotic pressure. Under this process the crystal continues to dissolve and the membrane surrounding it continues to stretch until the latter ruptures, ejecting a jet of fluid into the surrounding solution. At each of the points of rupture there develop tubular fibers. Under the right conditions, these can grow to many centimeters in length. Thus are formed the characteristic chemical-garden growths. Most metals, except the alkali metals of group 1 of the periodic table, whose silicates are very soluble, produce growths (12). The compositions of two silicate-garden precipitates have recently been studied in detail: those formed from aluminium nitrate (13, 14), and from copper nitrate (15). The former precipitate is a material with a hierarchical structure on the nanoscale, consisting of silica nanotubes clustered together over several orders, surrounded by aluminosilicate and aluminium hydroxide. The latter precipitate is more crystalline, being formed in part of crystalline copper hydroxide nitrate, together with amorphous silica.

Apart from their purely scientific fascination as spectacular examples of pattern formation, chemical gardens may be implicated in practical problems that involve the precipitation of a colloidal gel membrane separating two aqueous solutions of different compositions. The importance for cement technology arises from understanding the hydration of Portland cement. The chemistry involved in the formation of Portland cement may be

0021-9797/02 $35.00
© 2002 Elsevier Science (USA)
All rights reserved.

seen as a type of silicate-garden system (16–20). While in the usual silicate garden a crystal of a soluble metal salt is immersed in a solution of sodium silicate, in Portland cement solid calcium silicates are immersed in water and a membrane of calcium silicate hydrate is formed around them. Because of its semipermeable character, osmosis creates an excess pressure in the volume enclosed by the membrane that causes its rupture, and jets of solution are ejected that react with the outer solution to precipitate further material as thin tubular filaments of calcium silicate hydrate. The fabrication of the cement consists of the formation of a mesh of these filaments. The Portland cement system is then analogous to a reverse silicate garden, one in which sodium silicate grains are immersed in a metal ion solution. A further example of a possible practical application of chemical gardens is to metal corrosion in aqueous environments, in which corrosion products on the metal surface may be colloidal in character (21, 5, 11), and corrosion tubes can form on the surface of rusting iron or steel (40–44). Lastly, in lead–acid battery technology, a membrane–osmosis model of battery paste has been suggested (22). In an interesting example of the cyclic nature of science, a century on from the research of Leduc (1), Herrera (2), and others that linked chemical gardens to the origin of life through their similarity in morphology, the wheel has turned full circle. Recent work speculates that chemical-garden-type membranes produced in precipitates in submarine vents early in our planet's history would be natural containers within which the controlled environment may have provided the impetus for the emergence of life on Earth (23).

Investigations of chemical gardens have concentrated up to now on understanding the chemistry producing the membrane and the mechanism of its rupture. Here, we look at the physics giving rise to the pattern formation.

2. MATERIALS AND METHODS

We elected to maintain the same anion and cation in all our experiments and concentrate on the effects of changes in the other variables. We chose cobalt(II) chloride hexahydrate, $CoCl_2 \cdot 6H_2O$, as the metal salt we would use throughout and sodium silicate as the reacting solution. Aqueous sodium silicate solutions were prepared from a concentrated solution, 6.25 M with respect to silica, composed of ca. 27% SiO_2 and 14% NaOH, by diluting it with bidistilled water. We prepared aliquots of dilutions from 1 : 1 to 1 : 100 v/v, giving us concentrations between 6.25 and 0.0625 M with respect to silica.

For ease of data collection, we wished to have an approximately two-dimensional system. For this reason we performed the experiments in a 1-mm-thick Hele-Shaw cell (24, 25) of dimensions 1.5×2 cm formed by two parallel glass plates sealed at their edges. Changes in the solution refractive index observed with a Mach–Zehnder interferometer were used to follow the experiments. The solution refractive index is linked to composition; it varies approximately linearly with the concentration of a dissolved solute. We measured the refractive indices of sodium silicate and cobalt chloride solutions: the refractive index of 1.56 M sodium silicate solution is 1.35 and that of 0.781 M solution is 1.34, while a saturated 4.10 M solution of cobalt chloride has a refractive index of 1.41, and a 2.05 M solution has one of 1.37. A concentration gradient in a solution is then visible with the interferometer as a curving or bowing of the interference fringes.

The experimental procedure was to insert a seed crystal into the growth cell and, after placing the cell oriented vertically in the test arm of the interferometer, to fill the cell with sodium silicate solution using a syringe to begin the experiment (Fig. 2a).

Experiments were performed in a temperature-controlled laboratory maintained at $20 \pm 1^{\circ}$C.

3. MECHANISM OF GROWTH

Figure 1 presents a collection of photographs showing the typical forms of chemical gardens grown from a cobalt chloride crystal seed in various concentrations of sodium silicate solution. We now describe how these structures are seen to form and grow in our experiments.

3.1. Membrane Expansion and Rupture

As soon as the seed crystal comes into contact with the aqueous silicate solution, it begins to dissolve and at the same time is covered by a colloidal coating of cobalt silicate hydrate (Fig. 2b). This material acts as a semipermeable membrane, as hypothesized by Traube (7) and demonstrated in laboratory osmosis experiments using a supporting structure for the membrane by Pfeffer (4) and more recently by Coatman *et al.* (11). Figure 3 shows a sequence of interferograms taken seconds after the start of an experiment performed with a 0.781 M sodium silicate solution and a cobalt chloride crystal seed. As a consequence of the different osmotic pressures inside the membrane—a concentrated cobalt chloride solution—and outside—a solution of silicate depleted in the metal salt—water is drawn osmotically from outside into the membrane, permitting the further dissolution of the crystal (Fig. 2c). The entry of water causes the membrane to dilate under osmotic pressure—cf. Figs. 3a and 3b, taken at 14 and 18 s—until it ruptures (Fig. 2d). This provokes the injection of the salt solution in its interior into the silicate solution—cf. Fig. 3c, taken at 28 s. The membrane usually ruptures more than once, and so each seed crystal has several streams of liquid emanating from the membrane surrounding it.

Upon rupture of the membrane, liquid is ejected under pressure. It thus forms a submerged jet made up of cobalt chloride solution (Fig. 4a). This is less dense than the sodium silicate solution into which it emerges, so it tends to rise. After the initial rupture, the injection pressure drops, and the fluid flow becomes less like a jet and takes on the character of a buoyant plume. In other words, the nature of the flow changes as the experiment progresses from forced convection—a jet whose dynamics is dependent on the injection pressure from osmosis—initially, to free convection—a plume whose dynamics is dependent on its

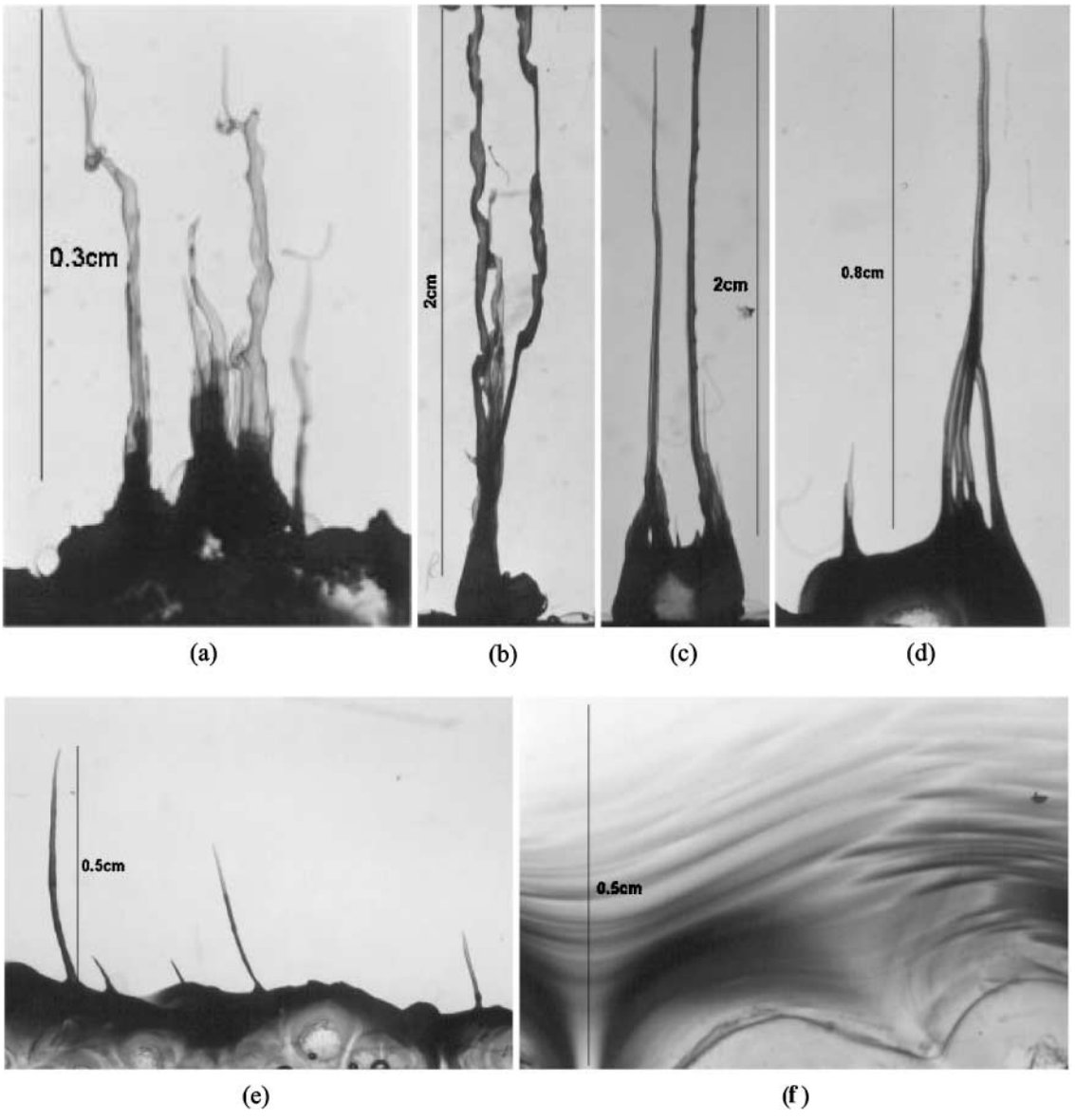

FIG. 1. Chemical gardens grown from a cobalt(II) chloride hexahydrate crystal seed and different sodium silicate solutions: (a) 6.25 M, (b) 1.04 M, (c) 0.625 M, (d) 0.313 M, (e) 0.156 M, and (f) 0.104 M.

buoyancy—finally. For this reason, while the jets formed on membrane rupture are at first at arbitrary angles to the vertical, over time they become reoriented until they end up pointing directly upward, when they are buoyant plumes, as we illustrate in Fig. 4.

3.2. Osmotic Pump and Tube Growth

At the edges of the jets or plumes, at the interface between the moving cobalt chloride solution and the stationary sodium silicate solution of the bulk, cobalt silicate is precipitated. This forms a gradually advancing roughly cylindrical wall around the fluid in motion, growing up from its base in the original membrane. Thus are formed the tubes characteristic of chemical gardens (Fig. 2e). Osmosis continues to drive the flow after the initial breakage of the membrane. Water flows into the growth mainly near the base, where the concentration of metal salt—and hence the osmotic pressure—is highest, and escapes out through the growing tubes, thus forming an osmotic pump in which inflow occurs over extensive regions of the membrane, while outflow is localized at the tube mouth. In the series of images in Fig. 4 appears a tube in formation in the same experiment that was depicted in Fig. 3. In interpreting these images it is useful to bear in mind that the variations in refractive index made visible by the curvature of the interference fringes occur in the liquid inside the tubes, and in the plumes emanating from them, because of changes in cobalt chloride concentration, whereas the variations in other regions outside the tubes occur as a result of changes in the sodium silicate concentration.

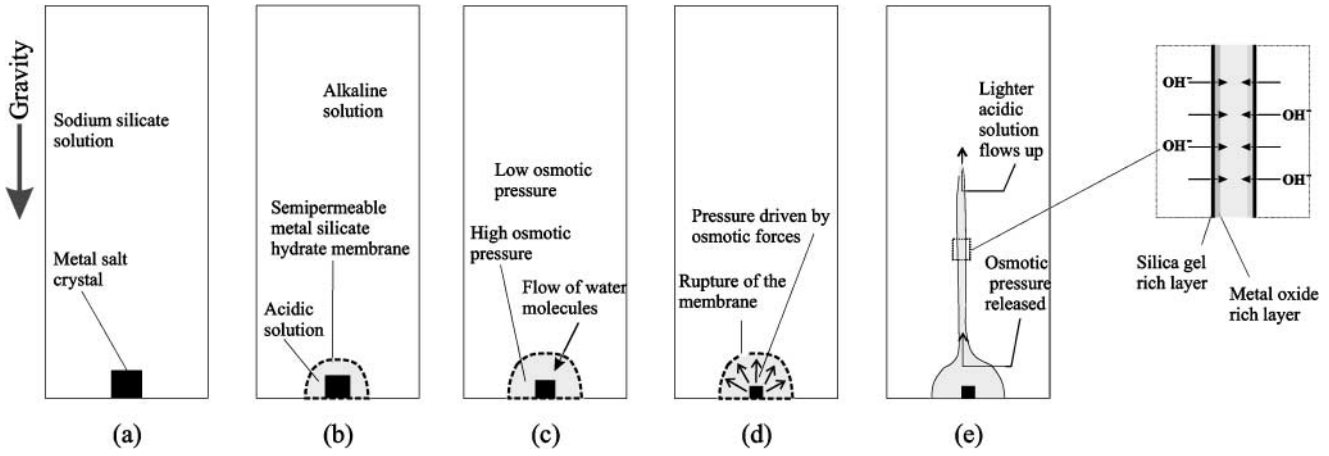

FIG. 2. Chemical-garden growth: (a) setup at start of the reaction, (b) membrane formation between acidic and basic solutions, (c) osmotic pressure is higher within membrane than outside it, so it expands, (d) under osmotic forces the membrane ruptures, and (e) a tube forms.

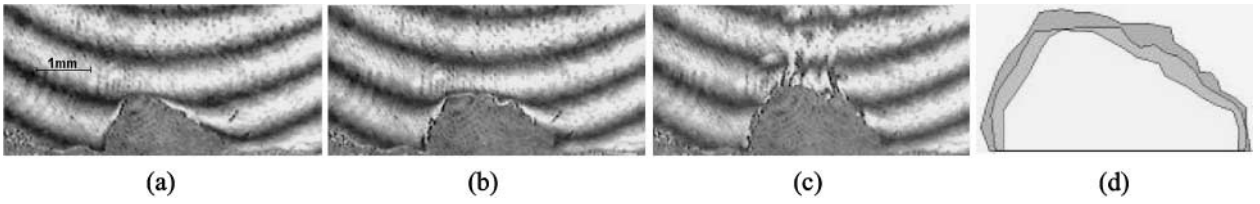

FIG. 3. The first stage of chemical-garden formation: membrane expansion and rupture. A sequence of interferograms—taken at (a) 14 s, (b) 18 s, and (c) 28 s—in an experiment performed with a 0.781 M sodium silicate solution. The membrane increases in volume like a balloon being inflated, as the diagram in (d), depicting the change from (a) light through (c) dark, shows, until it ruptures with the consequent injection of the solution of cobalt chloride into the sodium silicate solution.

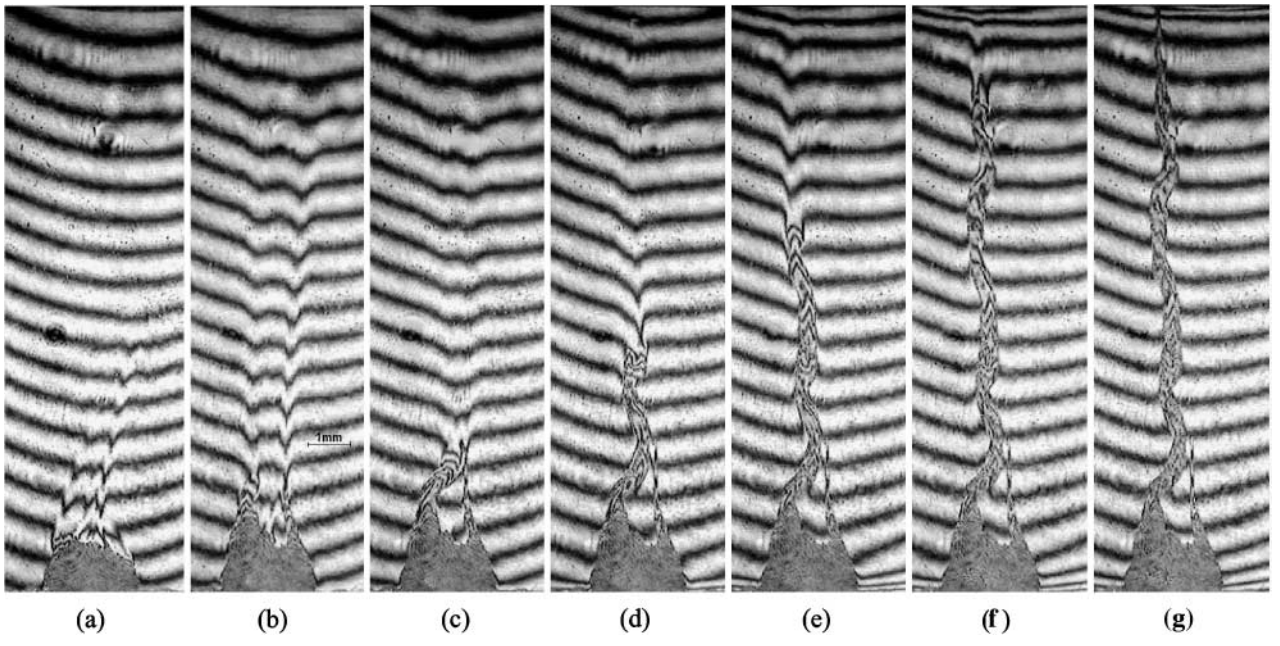

FIG. 4. The second stage of chemical-garden formation: tube growth. Interferometric images recorded at (a) 48 s, (b) 92 s, (c) 120 s, (d) 182 s, (e) 250 s, (f) 360 s, and (g) 600 s of the same experiment as in Fig. 3.

FIG. 5. A close-up view of part of Fig. 4e.

Observe the image in Fig. 4e, repeated in close-up in Fig. 5a. The plume emerging from the growing tube causes the fringes to curve downward, as the refractive index of cobalt chloride is larger than that of the surrounding sodium silicate solution. The plume is seen to be weaker—the bowing is less pronounced—at a greater distance from its source. Near to the outer surface of the tube in the regions away from its mouth, the fringes locally bow upward. This curvature, the effect of a decrease of the refractive index toward the tube, indicates that the local sodium silicate concentration is diminished there. This depletion zone is probably a consequence of the entry of hydroxide ions into the interior of the tube (26); the sodium silicate solution is basic. The latter in turn precipitates as silica on the outer wall, as its solubility decreases with decreasing pH (10), which reduces the sodium silicate solution concentration outside. Within the tube, on the other hand, as we follow the line of the tube back from its mouth, the direction of curvature of the fringes changes. In the region nearer the mouth, the fringes curve downward toward the walls, which indicates a greater refractive index there. This is probably a consequence of the cobalt silicate hydrate material that has precipitated to form the cylindrical wall having a refractive index higher than that of the solutions on either side; light traversing the tube will pass through a greater depth of this high-refractive-index material closer to the walls than in the center of the cylinder and produce this effect. In the region further from the mouth, the decrease in refractive index giving an upward curvature toward the walls may be due to the deposition of cobalt hydroxide on the inner wall, as the cobalt ions react with the hydroxide ions that have entered through the tube wall.

As liquid flows up the tube, it passes first through a well-mixed region at the base, followed by a region in which cobalt hydroxide is being deposited, and finally a region near the mouth in which the tube wall is being formed. The precipitation of different materials on the inner and outer tube surfaces must give a strong compositional gradient across the thickness of the tube wall (26). Moreover, this gradual deposition of material on the walls leads to the tubes becoming stiffer over time. This gradual aging of the precipitates continues even after the end of growth; they harden over time for several days or weeks. When the semipermeable membrane ruptures, a solution of cobalt chloride escapes across the break. But it does not precipitate immediately in the silicate solution. Precipitation can only occur if sufficient concentrations of both cobalt chloride and sodium silicate are present. The necessary conditions of concentration of both reagents are satisfied only at the interface between the jet or plume and the bulk, as the moving fluid is impoverished in sodium silicate, while in the bulk there is too little cobalt chloride. At the end of growth, by the same token, precipitation no longer occurs, as the flow up the tube is now too depleted in cobalt chloride.

Several mechanisms can contribute to changes in tube diameter. As a tube lengthens, there is a decrease in flow rate with increasing drag from its walls and a consequent tube diameter reduction. Sometimes there is an abrupt change in flow rate and in diameter induced by a fresh membrane rupture (11). Second, the osmotic pump mechanism maintaining flow up the tube decreases in intensity as the seed crystal dissolution rate is lowered. Tube growth ends when the flow of liquid up the tube abates. Either the crystal is now dissolving very slowly or has dissolved completely, and as the solution within the membrane is no longer near saturation, the osmotic pressure drops. As the flow weakens, the tube narrows in diameter; often it finally pinches off to a point (Fig. 4g). An additional mechanism that may contribute when the dimensions involved are sufficiently small is the force induced by Derjaguin–Landau–Verwey–Overbeek (DLVO) interactions (27, 28) between the tube walls.

3.3. Effects of Varying Concentrations

There is a spread of chemical combinations for which silica gardens develop. This indicates that their growth is not so much due to a special chemical composition as to the precipitation process and to physical characteristics of the precipitate. A range of pH causing a growth minimum was noted by Damerell and Brock (29), who supposed it to arise from changes in membrane permeability. We have confirmed—cf. Fig. 1—observations of Coatman *et al.* (11) that there is a range of optimal concentrations of sodium silicate in which growth is most vigorous. We find this to lie between 1.56 and 0.625 M with respect to silica in our experiments. The more concentrated solution in Fig. 1a is seen to produce meager growth, and there is vigorous growth for intermediate concentrations (Fig. 1b–1e) while the more dilute solution of Fig. 1f produces merely a gelatinous mass. Possibly, as Coatman *et al.* (11) hypothesize, in more concentrated

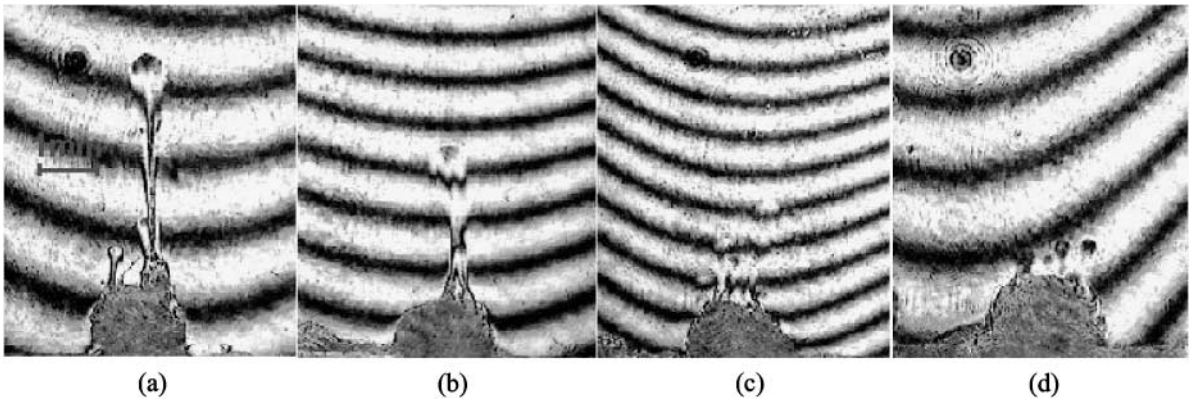

FIG. 6. Interferograms showing sodium silicate solutions of different concentrations (a) 1.56 M, (b) 1.04 M, (c) 0.781 M, and (d) 0.625 M at the same time—20 s—after the start of the experiment.

solutions of sodium silicate, the membrane surrounding the seed is broken only with difficulty to produce the growth of tubes. On the other hand, as the solution becomes more diluted, the membrane that is formed acquires a more plastic character and is not easily ruptured, but rather distends without breaking. In Fig. 6, experiments are shown at equal times from their start for varying concentrations. The sodium silicate concentrations used cover the range of optimal growth conditions. Within this range it is notable that the membrane ruptures earlier in more concentrated solutions.

The growth rate of a tube depends upon the flow rate of the osmotic pump, which in turn hinges on the difference in osmotic pressure across the semipermeable membrane between the interior and exterior solutions, and then on the dissolution rate of the crystal and the solubility of the metal salt (5). The resultant net osmotic pressure is always so as to dilate the membrane. The osmotic pressure within the membrane is almost constant if the solution is always nearly saturated, as is the case with cobalt chloride, saturated at approximately 4.1 M at 20°C. On the other hand, the osmotic pressure exerted by the silicate solution outside varies depending on its concentration. The increase of osmotic pressure with concentration is not linear in sodium silicate, however. As, in more concentrated solutions, much of the silicate is present as polymeric aggregates (10), the osmotic presssure is lower than if the silicate were not aggregated (5). This relatively low osmotic pressure of sodium silicate makes for a large osmotic pressure difference across the semipermeable membrane even in rather concentrated solutions, important for growing chemical gardens. Note that although we speak here throughout of a semipermeable membrane, its semipermeability will not be perfect, and there will be some transport of solute across it (1). Although in strong solutions the osmotic pressure difference is somewhat lower, it is under these conditions that the chemical reaction is most active and more membranous material is produced, while on the other hand, in weaker solutions, there is less silicate, and the reaction producing the membrane is less vigorous. In this way there is a complex interplay between osmosis and reaction.

More concentrated silicate solutions are denser than more dilute solutions. As the cobalt chloride solution ejected from within the membrane is lighter still, it rises. The density difference determines the buoyancy of the rising fluid; a critical parameter that conditions the nature of the convective flow in the form of a buoyant plume. The Rayleigh number Ra gives the ratio between buoyant and viscous forces, and thence the importance of convective effects. For solutal convection, $Ra_C = \rho g \beta_C \Delta C d^3/(\eta D)$, where ΔC is the change in concentration across the convecting layer, d the depth of the layer, η the viscosity of the liquid, D the molecular diffusivity, g the acceleration due to gravity, ρ the fluid density, and $\beta_C = 1/\rho \partial\rho/\partial C$ the volume expansion coefficient with concentration. For thermal convection, $Ra_T = \rho g \beta_T \Delta T d^3/(\eta\kappa)$, where ΔC is the change in temperature across the convecting layer, κ the thermal diffusivity, and $\beta_T = 1/\rho \partial\rho/\partial T$ the volume expansion coefficient with temperature. The relative importance of the two mechanisms of convection may be estimated with the ratio $Ra_C/Ra_T = \beta_C \Delta C/(\beta_T \Delta T) \cdot \kappa/D$, which may be written as $\Delta\rho_C/\Delta\rho_T \cdot \kappa/D$, where $\Delta\rho_C$, is the density change induced by concentration differences, and $\Delta\rho_T$ is the density change induced by temperature differences. Since molecular diffusivities are around a thousand times smaller than thermal diffusivities, $\kappa/D \sim 10^3$. Moreover, in these experiments the density differences arise almost entirely through concentration changes, and temperature changes play only a minor role: we can estimate $\Delta\rho_T/\rho \sim 10^{-5}$, while $\Delta\rho_C/\rho \sim 10^{-2}$. All of this means that $Ra_C/Ra_T \sim 10^6$, so solutal convection is overwhelmingly more important than thermal convection here.

When the density difference is greatest, in the most concentrated solutions, the plume is most intense. This is corroborated by Fig. 7, in which appear plumes from the same four concentrations as in Fig. 6, but this time for the moment corresponding to the most vigorous activity. From the experiments depicted in Fig. 7 we have extracted information on the velocity V of the cap of the rising plume associated with the different concentrations. Combining these data with measurements of the diameters L of the tubes at their mouths, and supposing the kinematic viscosity

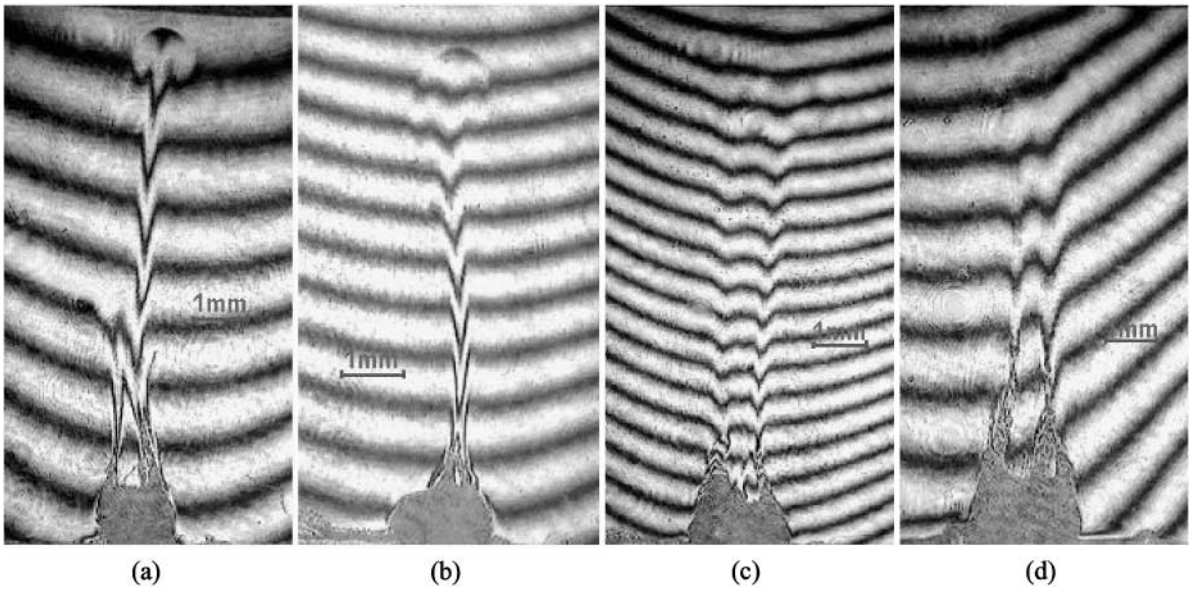

FIG. 7. Plumes of cobalt chloride solution are seen emerging after membrane rupture in interferometric images corresponding to sodium silicate solutions of (a) 1.56 M, at 30 s; (b) 1.04 M, at 30 s; (c) 0.781 M, at 86 s; and (d) 0.625 M, at 200 s.

ν of the fluid to be on the order of that of water, we may calculate the Reynolds numbers—$Re = VL/\nu$—involved. We find for 1.56 M, $Re = 0.08$; for 1.04 M, $Re = 0.06$; for 0.781 M, $Re = 0.02$; and for 0.625 M, $Re = 0.03$. This is to say that the more concentrated the silicate solution, the more intense the plume.

3.4. Instabilities of Tube Formation and Growth

The buoyant plumes around which tubes form rise straight up, but a glance at a chemical garden shows that the growths are often anything but straight. What is the cause of these tube instabilities?

In Fig. 7 the interface between the rising fluid and the stationary fluid surrounding it can be seen to have assumed the typical mushroom shape associated with the caps of convective plumes (30). In all the images of Fig. 7 there are multiple tubes. Each tube has an associated plume, and interactions between nearby plumes can be seen in several cases, in which two neighboring plumes coalesce to form a single larger plume, a phenomenon first studied by Rouse *et al.* (31) and later beautifully visualized in experiments by Pera and Gebhart (45), and Moses *et al.* (30). This process, which is a form of the Coanda effect (46), can be observed in the sequence of images in Fig. 4, in which it is seen that the attraction between neighboring plumes which leads to plume coalescence is a cause of the tubes curving together and joining, visible also in Fig. 1d.

Plume entrainment is not, however, the only reason for the instabilities in tube growth, as can be confirmed by a glance at Figs. 1 and 4, in which isolated tubes are also seen to be curved. The progression in Fig. 1 is particularly interesting, as it is noticeable that the tubes are more affected by growth instabilities at higher concentrations of silicate solution. There are various possible explanations for this. One hypothesis lies in the hose instability, familiar to gardeners and firemen alike, in which a straight flexible tube unsupported at its end is unstable to snaking for flow rates above a threshold (32). As we noted above, the plumes at higher silica concentrations are more intense, which is consistent with the curvature mechanism being a hose instability. Apart from this dynamical mechanism, another possibility is that stochastic variations in the deposition of new material around the wall may lead to the flow deviating from the straight ahead, giving rise to curvature of the tubes. Also, being denser than the surrounding medium, they can buckle under their own weight, which constitutes a third possible mechanism. Buckling sometimes leads to growing tubes breaking off completely and sinking to the bottom of the container. But, if a tube only partially breaks open, it can continue to grow both from its original end and from the new aperture. This provides a mechanism for tube branching, which appears to be common in the most brittle growths, while not seen in those that are more flexible.

3.5. Effects of Buoyancy

It is evident that buoyant plumes are a major feature of the dynamics of chemical gardens. This may be confirmed by orienting the Hele–Shaw growth cell horizontally rather than vertically or by placing a crystal at the surface of a solution of sodium silicate. If the latter operation is performed carefully, surface tension will keep the crystal from sinking. In this case, tubes do not form in solutions in which they would normally do so, and instead the growth is in the form of a cup around the underside of the crystal, as Fig. 8a demonstrates, which may gradually be enlarged downward by the osmotically driven flow of liquid into it (5). Furthermore, if the crystal is attached to the wall of the chamber, as shown in Fig. 8b, instead of being placed at its base, tubes grow from it as normal, but only upward and not downward.

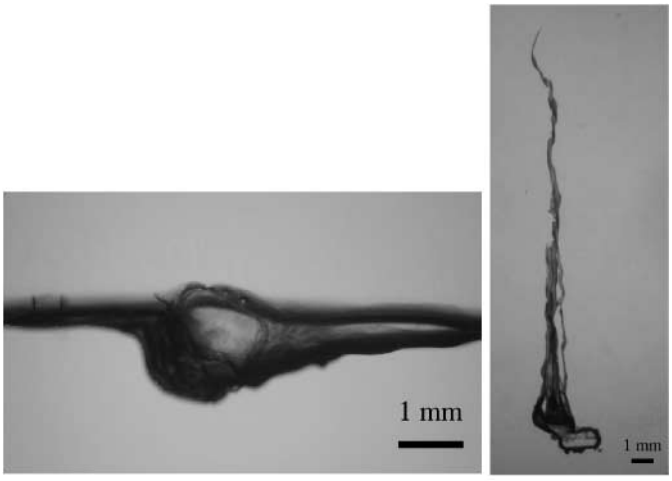

FIG. 8. (a) Growth formed by a crystal placed at the surface of a 0.781 M sodium silicate solution, showing that in this configuration tubes are not formed. (b) Growth formed by a crystal attached to the wall of the chamber, showing that the tubes grow upward but not downward.

If the effects of buoyancy are removed, the remaining driving force for chemical-garden formation is osmotic pressure, which dilates the initial membrane and powers the jet of fluid that emerges under pressure from a break. This naturally leads one to ask what form a chemical garden would take in the absense of buoyancy; or what is the same thing in the absense of gravity. We should expect to find that free convection (buoyant plumes) has disappeared, and there remains only forced convection (osmotically powered jets). Chemical-garden experiments have been performed at least twice under microgravity conditions, in which they can be studied in three dimensions. Stockwell and Williams (33) report growth in random directions, together with spirals for which they had no explanation. Unfortunately they provide few details of their experiments. Subsequently Jones and Walter (26, 39) flew a further experiment, in which they found that the reaction occurred an order of magnitude slower than on ground, due to the absence of free convection. The absence of buoyancy-driven flow led to novel structures, as apart from the tubes seen on Earth, they found also evidence for spherical membranes and fingers, structures typical of Laplacian growth mechanisms such as viscous fingering. A preliminary model for the instability of a moving semipermeable membrane as may be applied to this case has been presented by Sørensen (34).

4. DISCUSSION

It is interesting to speculate whether under ideal conditions—with an initially homogeneous membrane—the tube spacing might be determined by a dynamical instability. The model put forward by Sørensen (34) attempted to address this question, but found no such characteristic wavelength of instability. Sørensen suggested that the addition of additional factors to his model might provide the answer, and Jones and Walter (26) speculated as to the physical mechanism that might lead to such an instability. In the initial stages of chemical-garden membrane formation and expansion, especially if buoyancy may be suppressed, as in microgravity, molecular transport is diffusive rather than convective. The chemical-garden system may be considered as a flexible self-renewing semipermeable membrane that hardens slowly and is subjected to osmotic pressure. A flat membrane, or one with constant curvature, may become unstable under internal pressure, as a slightly more flexible region will form a bulge and in the process become thinner, be renewed by diffusion with fresh membranous material, and thence weaken further and develop into a finger. This describes the instability of Laplacian growth first noted by Mullins and Sekerka (35), and so chemical-garden tube formation would be related to viscous fingering, dendritic growth, and dielectric breakdown among many other systems describable with the Laplace equation. However, although it is appealing to consider, in the actual experiments the membrane is rather inhomogeneous and ruptures at its weakest points, so there is no evidence of this. With other reagents a characteristic spacing of tubes may be more apparent (cf. Fig. 2 of Double and Hellawell (16) and Fig. 1 of Coatman *et al.* (11), both obtained with cobalt nitrate).

There are a couple of phenomena commonly noted in work on chemical gardens that we have not yet mentioned. Leduc (1), Hazlehurst (5), and others have observed segmentation and striation patterns on chemical-garden tubes. These appear to derive from a periodic growth mechanism for a tube that forms not by continuous accretion at its open end, but as a series of vesicles that accumulate in line by membrane formation and rupture. We have occasionally observed some such segmentation effects, but they are not present in the experiments shown here. Possibly they require weaker osmotic and convective processes that may be produced with different reagents. Hazlehurst (5) proposes that the main mechanism of tube growth involves a gas bubble trapped in the tube mouth. We have not observed such bubbles in our work. The reason for this may be that we performed our experiments in a closed growth cell, while his were open to the atmosphere. Although if they are present they may accelerate tube growth, our work shows that gas bubbles are not necessary components for chemical-garden formation.

Chemical-garden experiments have long been used to excite the interest of the nonscientific public in chemistry and are included in most chemistry sets for children (36). They have even entered literature, being mentioned in Thomas Mann's novel *Doktor Faustus* (47). It is ironic, then, that this first introduction to chemistry is a complex phenomenon not fully understood after more than a century of study. Our aim in this work has been to carry a step forward the knowledge of the mechanisms involved in forming these fascinating patterns. From Leduc's *synthetic biology* (1), Herrera's *plasmogeny* (2), and others pursuing similar researches—see Chapter 10 of Leduc's book for a review of the investigators then active in the field and their findings—came studies of chemical-garden growths imitating many natural forms: stems, leaves, twigs, roots, shells, mushrooms

and other fungi, flowers, amoebae, and worms. These they produced by varying the composition and concentrations of the reacting solutions during the growth phase. They were searching for the origin of life, an end that as we now understand could not be achieved without a knowledge of biochemistry. Their research, although now nearly forgotten, was not however in vain. Their accurate descriptions of chemical-garden formation are as valid today as a century ago. Leduc argued that the formations were osmotic growths, while Herrera maintained that buoyancy forces were the critical component. We have shown here that, on Earth at least, chemical gardens result from a combination of these two mechanisms.

ACKNOWLEDGMENTS

This investigation was conceived by J.M.G.R., while M.L.N. performed the experimental work as part of her doctoral thesis (37) completed in 2000 under the supervision of J.M.G.R. and F.O., and J.H.E.C. performed the analysis of the fluid and tube dynamics. We thank Ignacio Sainz, Oliver Steinbock, and Ana Villacampa for useful conversations, and Eva Herrera for help with the experimental work. J.H.E.C. acknowledges the financial support of the Spanish CSIC, Plan Nacional del Espacio contract PNE-007/2000-C, and M.L.N. acknowledges an ESA fellowship.

REFERENCES

1. Leduc, S., "The Mechanism of Life." Rebman, London, 1911.
2. Herrera, A. L., "Boletin de la Dirección de Estudios Biológicos, México," Volume 1–2. 1916–1917.
3. Zeleny, M., Klir, J., and Hufford, K. D., *in* "Artificial Life: SFI Studies in the Sciences of Complexity" (C. Langton, Ed.), pp. 125–139. Addison–Wesley, Reading, MA, 1988.
4. Pfeffer, W., "Osmotic Investigations." Van Nostrand–Reinhold, New York, 1985.
5. Hazlehurst, T. H., *J. Chem. Educ.* **18,** 286–289 (1941).
6. Copisarow, M., *J. Chem. Soc.* 222–234 (1927).
7. Traube, M., *Arch. Anat. Physiol.* 87–165 (1867).
8. Wald, G., *J. Chem. Educ.* **63,** 658–659 (1986).
9. van't Hoff, J. H., *Z. Phys. Chem.* **1,** 481–508 (1887).
10. Dent Glasser, L. S., *Chem. Br.* **18,** 33–39 (1982).
11. Coatman, R. D., Thomas, N. L., and Double, D. D., *J. Mater. Sci.* **15,** 2017–2026 (1980).
12. Clunies Ross, W. J., *J. R. Soc. N. S. Wales* **44,** 583–592 (1910).
13. Collins, C., Zhou, W., Mackay, A. L., and Klinowski, J., *Chem. Phys. Lett.* **286,** 88–92 (1998).
14. Collins, C., Mann, G., Hoppe, E., Duggal, T., Barr, T. L., and Klinowski, J., *Phys. Chem. Chem. Phys.* **1,** 3685–3687 (1999).
15. Collins, C., Zhou, W., and Klinowski, J., *Chem. Phys. Lett.* **306,** 145–148 (1999); see Erratum, *Chem. Phys. Lett.* **312,** 346 (1999).
16. Double, D. D., and Hellawell, A., *Nature* **261,** 486–488 (1976).
17. Double, D. D., and Hellawell, A., *Sci. Am.* **237,** 82–92 (1977).
18. Double, D. D., Hellawell, A., and Perry, S. J., *Proc. R. Soc. London A* **359,** 435–451 (1978).
19. Birchall, J. D., Howard, A. J., and Bailey, J. E., *Proc. R. Soc. London A* **360,** 445–453 (1978).
20. Double, D. D., *Philos. Trans. R. Soc. London. A* **310,** 55–63 (1983).
21. Lillie, R. S., and Johnston, E. N., *Biol. Bull.* **36,** 225–272 (1919).
22. Julian, K., *J. Power Sources* **11,** 47–61 (1984).
23. Russell, M. J., and Hall, A. J., *J. Geol. Soc. Lond.* **154,** 377–402 (1997).
24. Hele-Shaw, H. S., *Nature* **58,** 33–36 (1898).
25. Saffman, P. G., and Taylor, G., *Proc. R. Soc. London A* **245,** 312–329 (1958).
26. Jones, D. E. H., and Walter, U., *J. Colloid Interface Sci.* **203,** 286–293 (1998).
27. Derjaguin, B. V., and Landau, L., *Acta Physicochim. USSR* **14,** 633–662 (1941).
28. Verwey, E. J.W., and Overbeek, J. T. G., "Theory of Stability of Lyophobic Colloids." Elsevier, Amsterdam, 1948.
29. Damerell, V. R., and Brock, H., *J. Chem. Educ.* **26,** 148 (1949).
30. Moses, E., Zocchi, G., Procaccia, I., and Libchaber, A., *Europhys. Lett.* **14,** 55–60 (1991).
31. Rouse, H., Baines, W. D., and Humphreys, H. W., *Proc. Phys. Soc. B* **66,** 393–399 (1953).
32. Païdoussis, M. P., and Li, G. X., *J. Fluids Struct.* **7,** 137–204 (1993).
33. Stockwell, B., and Williams, A., *School Sci. Rev.* **76,** 7–14 (1994).
34. Sørensen, T. S., *J. Colloid Interface Sci.* **79,** 192–208 (1981).
35. Mullins, W. W., and Sekerka, R. F., *J. Appl. Phys.* **35,** 444–451 (1964).
36. Webster, M., *Educ. Chem.* **35,** 126 (1998).
37. Novella, M. L., "Caracterización por Interferometría Mach–Zehnder de Procesos de Crecimiento de Cristales a Partir de Soluciones." Ph.D. thesis, University of Granada, 2000.
38. Glauber, J. R., "Furni Novi Philosophici,", Amsterdam, 1646.
39. Jones, D. E. H., *Am. Sci.* **90,** 454–461 (2002).
40. Ackermann, A., *Kolloid Z.* **28,** 270–281 (1921).
41. Ackermann, A., *Kolloid Z.* **59,** 49–55 (1932).
42. Riggs, O. L., Sudbury, J. D., and Hutchison, M., *Corrosion* **16,** 260–264 (1960).
43. Sudbury, J. D., Riggs, O. L., and Radd, F. J., *Corrosion* **18,** 8–25 (1962).
44. Fontana, M. G., "Corrosion Engineering," McGraw-Hill, New York, third edition, 1986.
45. Pera, L., and Gebhart, B., *J. Fluid Mech.* **68,** 259–271 (1975).
46. Tritton, D. J., "Physical Fluid Dynamics," Oxford University Press, Oxford, second edition, 1988.
47. Mann, T., "Doktor Faustus," 1947.